

Reaction of $(\mu\text{-H})_2\text{Os}_3(\text{CO})_9(\text{PPh}_3)$ with Acetylene and Ethylene. Structures, Dynamics, and Interconversion of Two Isomers of the Vinyl Complex $(\mu\text{-H})\text{Os}_3(\text{CO})_9(\text{PPh}_3)(\mu\text{-CH}=\text{CH}_2)$

Makoto Koike, David H. Hamilton, Scott R. Wilson, and John R. Shapley*

School of Chemical Sciences, University of Illinois, Urbana, Illinois 61801

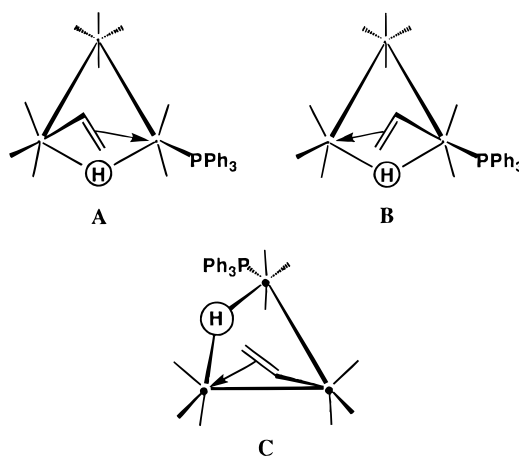
Received August 12, 1996[⊗]

As reported previously by Brown and Evans, the reaction of $(\mu\text{-H})_2\text{Os}_3(\text{CO})_9(\text{PPh}_3)$ with acetylene provides two isomers of the hydrido vinyl compound $(\mu\text{-H})\text{Os}_3(\text{CO})_9(\text{PPh}_3)(\mu\text{-}\eta^2\text{-CH}=\text{CH}_2)$ (**2**). The solid-state structures of these two isomers now have been defined by single-crystal X-ray crystallography. The major isomer **2a** contains a triangular array of osmium atoms with the vinyl ligand bridging the Os(2)–Os(3) edge, forming a σ -bond to Os(3) and a π -bond to Os(2), and the triphenylphosphine ligand coordinating to Os(2) in an “in-plane” position. The presence of the hydride ligand also bridging the Os(2)–Os(3) edge was deduced indirectly. The minor isomer **2b** also contains a triangular Os₃ array with the vinyl ligand bridging the Os(2)–Os(3) edge and forming a σ -bond to Os(2) and a π -bond to Os(3). The triphenylphosphine ligand is bound to Os(1). The presence of the bridging hydride on the Os(1)–Os(3) edge was not directly detected but was supported by analysis of the structure; the hydride ligand therefore does not bridge the same edge as the vinyl moiety. The solution structures and dynamics of **2a** and **2b** have been investigated by variable-temperature ¹³C NMR and ¹³C spin saturation transfer experiments; isomer **2a** exhibits evidence for nondegenerate σ/π bond interchange in the bridging vinyl group. Separation of **2a** and **2b** can be effected by thin-layer chromatography (silica; CH₂Cl₂/C₆H₁₄, 1:3); subsequent ¹H NMR spectra reveal slow equilibration of **2a** and **2b** (*t*_{1/2} = 85 min, **2a**:**2b** = 2.2:1 at equilibrium). The same mixture of isomers is formed from the reaction of **1** with ethylene at high pressure (500 psig), with the previously characterized complex $(\mu\text{-H})_2\text{Os}_3(\text{CO})_9(\text{PPh}_3)(\mu\text{-CHCH}_3)$ as an intermediate.

Introduction

The reactions of $(\mu\text{-H})_2\text{Os}_3(\text{CO})_{10}$ with unsaturated hydrocarbons and related substrates provide a host of organotriosmium cluster derivatives.¹ A natural question is the effect of phosphorus ligand substitution on the reactivity of $(\mu\text{-H})_2\text{Os}_3(\text{CO})_{10}$, and a number of $(\mu\text{-H})_2\text{Os}_3(\text{CO})_9(\text{PR}_3)$ derivatives have been examined.² Specifically, the reaction of $(\mu\text{-H})_2\text{Os}_3(\text{CO})_9(\text{PR}_3)$ (PR₃ = PPh₂Et, PPh₃, P(OMe)₃) with acetylene (1 atm) at room temperature was reported to form two isomers of the vinyl complex $(\mu\text{-H})\text{Os}_3(\text{CO})_9(\text{PR}_3)(\mu\text{-}\eta^2\text{-CH}=\text{CH}_2)$, which

were assigned structures A and B on the basis of ¹H



and limited ¹³C NMR evidence.³ However, these two structures are interconvertible by the σ,π -vinyl interchange process established previously for the parent compound $(\mu\text{-H})\text{Os}_3(\text{CO})_{10}(\mu\text{-}\eta^2\text{-CH}=\text{CH}_2)$ (**1**),⁴ and we were intrigued by the apparent dramatic difference in the energetics of this process for these simple derivatives. We have reinvestigated the reaction of $(\mu\text{-H})_2\text{Os}_3$

[⊗] Abstract published in *Advance ACS Abstracts*, October 15, 1996.

(1) (a) Deeming, A. J. *Adv. Organomet. Chem.* **1986**, *26*, 1. (b) *Gmelin Handbook of Inorganic Chemistry*; Springer-Verlag: New York, 1994; Organosmium Compounds, Parts B3 and B5.

(2) (a) Adams, R. D.; Selegue, J. P. *J. Organomet. Chem.* **1980**, *195*, 223. (b) Adams, R. D.; Golembeski, N. M.; Selegue, J. P. *J. Am. Chem. Soc.* **1981**, *103*, 546. (c) Adams, R. D.; Golembeski, N. M.; Selegue, J. P. *Inorg. Chem.* **1981**, *20*, 1242. (d) Adams, R. D.; Katahira, D. A.; Yang, L.-W. *J. Organomet. Chem.* **1981**, *219*, 85. (e) Feighery, W. G.; Allendoerfer, R. D.; Keister, J. B. *Organometallics* **1990**, *9*, 2424. (f) Glavee, G. N.; Daniels, L. M.; Angelici, R. J. *Organometallics* **1989**, *8*, 1856. (g) Deeming, A. J.; Donovan-Mtunzi, S.; Kabir, S. E.; Arce, A. J.; De Sanctis, Y. *J. Chem. Soc., Dalton Trans.* **1987**, 1457. (h) Deeming, A. J.; Fuchita, Y.; Hardcastle, K.; Henrick, K.; McPartlin, M. *J. Chem. Soc., Dalton Trans.* **1986**, 2259. (i) Deeming, A. J.; Manning, P. J.; Rothwell, I. P.; Hursthouse, M. B.; Walker, N. P. C. *J. Chem. Soc., Dalton Trans.* **1984**, 2039. (j) Burgess, K.; Holden, H. D.; Johnson, B. F. G.; Lewis, J.; Hursthouse, M. B.; Walker, N. P. C.; Deeming, A. J.; Manning, P. J.; Peters, R. *J. Chem. Soc., Dalton Trans.* **1985**, 85. (k) Bryan, E. G.; Jackson, W. G.; Johnson, B. F. G.; Kelland, J. W.; Lewis, J.; Schorpp, K. T. *J. Organomet. Chem.* **1976**, *108*, 385. (l) Kabir, S. E.; Rosenberg, E.; Day, M.; Hardcastle, K. I.; Walt, E.; McPhillips, T. *Organometallics* **1995**, *14*, 721. (m) Koike, M.; Shapley, J. R. *J. Organomet. Chem.* **1994**, *470*, 199.

(3) Brown, S. C.; Evans, J. *J. Chem. Soc., Dalton Trans.* **1982**, 1049.

(4) (a) Shapley, J. R.; Richter, S. I.; Tachikawa, M.; Keister, J. B. *J. Organomet. Chem.* **1975**, *94*, C43. (b) Keister, J. B.; Shapley, J. R. *J. Organomet. Chem.* **1975**, *85*, C29.

$(\text{CO})_9(\text{PPh}_3)$ with acetylene, and single-crystal X-ray diffraction studies of both isomers of $(\mu\text{-H})\text{Os}_3(\text{CO})_9(\text{PPh}_3)(\mu,\eta^2\text{-CH=CH}_2)$ (**2a**, **2b**) reveal that the major isomer **2a** indeed adopts structure A but that the minor isomer **2b** has structure C in the solid state. Solution ^{13}C NMR studies of these compounds provide evidence that the solid-state structures are adopted also in solution and, in addition, that structure B is indeed accessible from A by the σ,π -vinyl interchange process. However, a previously unsuspected equilibration of **2a** and **2b** has been observed. Furthermore, the same mixture of **2a** and **2b** has been prepared by treating $(\mu\text{-H})_2\text{Os}_3(\text{CO})_9(\text{PPh}_3)$ with ethylene (500 psig); an intermediate in this overall reaction, namely $(\mu\text{-H})_2\text{Os}_3(\text{CO})_9(\text{PPh}_3)(\mu\text{-CHCH}_3)$, has been the subject of an earlier study.^{2m}

Experimental Section

Materials. $(\mu\text{-H})_2\text{Os}_3(\text{CO})_9(\text{PPh}_3)$ was prepared by the literature method.⁵ $\text{Os}_3(\text{CO})_{12}$ was enriched by stirring a solution in decalin for 3 days at 120 °C in the presence of 12 equiv of ^{13}C O (Isotec, 99%). *n*-Hexane was treated with sulfuric acid and then distilled from sodium/potassium alloy before use.

Preparation of $(\mu\text{-H})\text{Os}_3(\text{CO})_9(\text{PPh}_3)(\mu\text{-}\eta^2\text{-CH=CH}_2)$ with Acetylene. A stirred solution of $(\mu\text{-H})_2\text{Os}_3(\text{CO})_9(\text{PPh}_3)$ (40 mg) in *n*-hexane at room temperature was treated overnight with a slow stream of acetylene, which had been passed through a trap of sulfuric acid and then a column of magnesium sulfate. The solvent was removed under reduced pressure, and the residue was recrystallized from methanol (yield ca. 30 mg). Characterization data (FD-MS, IR ($\nu(\text{CO})$), and ^1H NMR) obtained for the product $(\mu\text{-H})\text{Os}_3(\text{CO})_9(\text{PPh}_3)(\mu\text{-}\eta^2\text{-CH=CH}_2)$ were in close agreement with those reported by Brown and Evans.³ The two isomers **2a** and **2b** were obtained in the ratio 2.2:1, whereas the previous workers reported a ratio near unity. The ^{13}C NMR studies were conducted on the mixture as synthesized.

Preparation of $(\mu\text{-H})\text{Os}_3(\text{CO})_9(\text{PPh}_3)(\mu\text{-}\eta^2\text{-CH=CH}_2)$ with Ethylene. A 500 mL pressure bottle was charged with a solution of $(\mu\text{-H})_2\text{Os}_3(\text{CO})_9(\text{PPh}_3)$ (33 mg) in olefin-free *n*-hexane. After it was flushed with ethylene three times, the bottle was pressurized to 30 psig, and the solution was stirred for 2 days at room temperature. After the bottle was vented, the presence of $(\mu\text{-H})_2\text{Os}_3(\text{CO})_9(\text{PPh}_3)(\mu\text{-CHCH}_3)$ and unreacted $(\mu\text{-H})_2\text{Os}_3(\text{CO})_9(\text{PPh}_3)$ was determined by IR ($\nu(\text{CO})$).³ This solution was then transferred to a 500 mL autoclave that was pressurized with ethylene to 500 psig. The solution was stirred at room temperature overnight (16 h), and then the autoclave was vented. The solution was evaporated under reduced pressure, and the residue was purified by thin-layer chromatography, with 25% CH_2Cl_2 /75% *n*-hexane as eluent. The product mixture of **2a/2b** (25 mg, 75%) was characterized by its IR ($\nu(\text{CO})$) and ^1H NMR spectra.³

Separation and Reequilibration of Isomers 2a and 2b. The mixture of **2a** and **2b** was subjected to careful thin-layer chromatography, with CH_2Cl_2 /*n*- C_6H_{14} (1:3) as eluent. Two narrowly separated bands were observed, which were extracted from the silica gel with CH_2Cl_2 , and the solutions were quickly evaporated to dryness. The residues were dissolved in CDCl_3 , and the ^1H NMR spectra of the samples were recorded. One sample showed largely (ca. 90%) the resonances due to **2a** (δ 7.89 t, 4.37 d, 2.29 t, -18.91 d) and very little (ca. 10%) of the signals due to **2b** (8.95 dd, 5.30 d, 2.47 d, -19.06 d), whereas the other sample showed slightly less **2a** (40%) than **2b** (60%). Over time the signals due to **2b** increased in the first sample and decreased in the second sample, and after 2 days both samples showed the same **2a:2b** ratio of 2.2:1.

Repeating the separation procedure produced an essentially pure sample of **2a**, and the growth of the hydride ^1H NMR signal due to **2b** was followed at 22 °C. Analysis of the data as a reversible reaction with $K = 2.2$ gave $k_1 = 5.9 \times 10^{-3} \text{ min}^{-1}$ and $k_{-1} = 2.7 \times 10^{-3} \text{ min}^{-1}$.

^{13}C NMR Spectroscopy. ^{13}C NMR spectra with ^{13}C -enriched samples were recorded on a General Electric GN-500 spectrometer equipped with an NIC 1280 computer. Solutions for the ^{13}C NMR experiments were prepared in deuterated toluene, degassed by freeze-pump-thaw sequences, and sealed under vacuum. Chemical shifts were referenced to the para carbon resonance of toluene- d_8 at δ 137.5. Selective ^1H -decoupled ^{13}C NMR experiments were carried out at -70 °C by the gated-decoupled pulse sequence. A standard COSY pulse sequence with additional delays of 50 ms was used. The data matrix was acquired with 512 data points in t_1 and 1024 data points in t_2 . A total of 64 1D spectra along the t_1 dimension were collected. Apodization was applied to all data sets with 0.5 Hz exponential line broadening followed by a 10° shifted sine bell. The frequency domain matrices were symmetrized along the $F_1 = F_2$ diagonal. For ^{13}C spin saturation transfer experiments, a directional coupler was inserted between the output of the transmitter and the probe and the power reflected back from the probe due to ^{13}C decoupling was monitored during the course of the experiments. The ^{13}C decoupling power was adjusted by running selectively ^{13}C and broad-band ^1H -decoupled ^{13}C NMR spectra so that resonances close to the selective irradiation were unaffected. Selectivity of 100 Hz or less was achieved.

Crystallographic Analysis. Crystals of **2a** suitable for diffraction analysis were obtained by slow crystallization from methanol solutions at -20 °C in an NMR tube. Crystals of **2b** were obtained from pentane solutions cooled to -20 °C in an NMR tube. All diffraction measurements were made on a Syntex P2 four-circle diffractometer equipped with Crystal Logic automation using graphite-monochromatized $\text{Mo K}\alpha$ radiation. Details are summarized in Table 1.

The structure **2a** was solved by Patterson methods (SHELXS-86). The positions of the osmium atoms were deduced from a vector map. Least-squares-difference Fourier calculations revealed positions for the remaining non-hydrogen atoms. Hydrogen atoms were included as fixed contributors in "idealized" positions, except for H(41a), H(41b), H(42), and the hydrogen bridging Os(2) and Os(3), which were not included in structure factor calculations. In the final cycle of least squares, non-hydrogen atoms were refined with anisotropic thermal coefficients, and a group isotropic thermal parameter was varied for the hydrogen atoms. Convergence was indicated by the maximum shift/error for the last cycle. The highest peaks in the final difference Fourier map were in the vicinity of the osmium atoms. A final analysis of variance between observed and calculated structure factors showed no apparent systematic errors.

The structure of **2b** was solved by direct methods (SHELXS-86). The positions of the osmium atoms were deduced from an *E* map. Subsequent least-squares-difference Fourier calculations revealed positions for the remaining non-hydrogen atoms. The C(21)-O(21) carbonyl was refined as a rigid group. Hydrogen atoms were included as fixed contributors in "idealized" positions. H(41a), H(41b), H(42), and the hydrogen between the osmiums were not included in structure factor calculations. In the final cycle of least squares, isotropic thermal coefficients were refined for C(21) and the phenyl carbon atoms, whereas anisotropic thermal coefficients were refined for the remaining non-hydrogen atoms. Successful convergence was indicated by the maximum shift/error for the last cycle. The highest peak in the final difference Fourier map was in the vicinity of Os(1), possibly indicating a slight disorder around Os(1), C(41), and C(42). A final analysis of variance between observed and calculated structure factors showed no apparent systematic errors.

Table 1. Crystallographic Data for the Two Isomers of $(\mu\text{-H})\text{Os}_3(\text{CO})_9(\text{PPh}_3)(\mu\text{-}\eta^2\text{-CH=CH}_2)$ (2a,b**)**

	2a	2b
(a) Crystal Parameters		
chem formula	$\text{C}_{29}\text{H}_{19}\text{O}_9\text{Os}_3\text{P}$	$\text{C}_{29}\text{H}_{19}\text{O}_9\text{Os}_3\text{P}$
fw	1113.04	1113.04
cryst syst	triclinic	triclinic
space group (No.)	$P\bar{1}$ (No. 2)	$P\bar{1}$ (No. 2)
<i>a</i> (Å)	10.075(5)	11.305(2)
<i>b</i> (Å)	12.718 (4)	16.111(2)
<i>c</i> (Å)	13.054(4)	8.804(4)
α (deg)	113.05(1)	97.304(4)
β (deg)	93.50(1)	100.943(4)
γ (deg)	93.43(1)	72.943(4)
<i>V</i> (Å ³)	1530(1)	1499.2(7)
<i>Z</i>	2	2
D_{calcd} (g/cm ³)	2.416	2.465
μ (cm ⁻¹)	125.41	127.98
size (mm)	0.2 × 0.3 × 0.4	0.04 × 0.1 × 0.2
color	orange	yellow

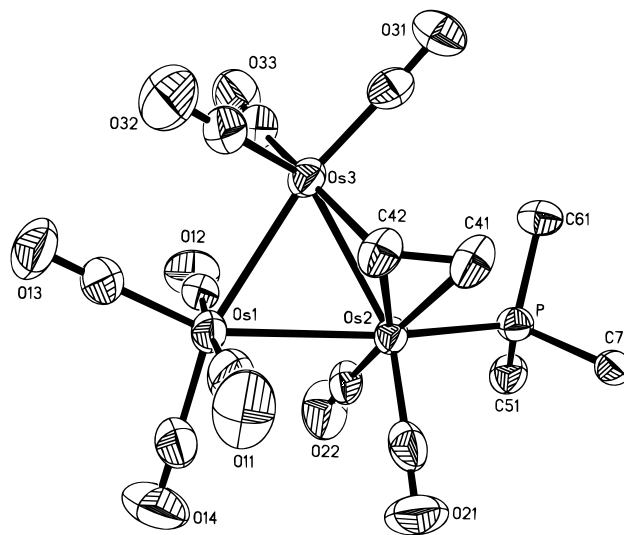
(b) Data Collection		
<i>T</i> (°C)	26	26
diffractometer	syntex P2 ₁	syntex P2 ₁
radiation	Mo K α	Mo K α
wavelength (Å)	0.710 73	0.710 73
monochromator	graphite	graphite
scan method	$\omega/2\theta$	$\omega/2\theta$
scan range (deg)	$3.0 \leq 2\theta \leq 34.0$	$3.0 \leq 2\theta \leq 30.0$
scan speed (deg/min)	5	5
no. of rflns measured	$+h, \pm k, \pm l$	$\pm h, \pm k, \pm l$
no. of rflns collected	4519	3155
indpdnt rflns	3977	2500
<i>R</i> (int)	0.042	0.033
no. of obsd rflns ($I > 2.58\sigma(I)$)	3522	2049
std rflns	3 std/100 rflns	3 std/100 rflns
transmission coeff	0.035–0.141	0.150–0.615

(c) Refinement ^a		
<i>R</i>	0.037	0.035
<i>R_w</i>	0.052	0.041
GOF or <i>E</i>	1.51	1.31
<i>k</i>	3.13	2.57
<i>p</i> factor	0.020	0.010
<i>N_o/N_v</i>	9.24	7.18
$\Delta\sigma$ (final)	0.001	0.003
$\Delta(r)$, e Å ⁻³	-1.86 to +2.00	-1.06 to +2.05

^a $R = \sum ||F_o| - |F_c|| / \sum |F_o|$; $R_w = (\sum w(|F_o| - |F_c|)^2 / \sum w|F_o|^2)^{1/2}$; $w = k / ((\sigma(F_o))^2 + [pF_o]^2)$; GOF or *E* = $(\sum w(|F_o| - |F_c|)^2 / (N_o - N_v))^{1/2}$.

Results and Discussion

Crystal Structure of 2a. The solid-state structure of **2a** was determined by single-crystal X-ray crystallography, and an ORTEP diagram of the molecule is shown in Figure 1. Important bond distances and angles are collected in Tables 2 and 3, respectively. The cluster contains a triangular array of osmium atoms, as expected, and the vinyl ligand bridges the Os(2)–Os(3) edge, forming a σ -bond to Os(3) and a π -bond to Os(2). The phosphine ligand coordinates in an in-plane or equatorial position on Os(2). Os(2) and Os(3) are associated with two and three terminal carbonyls, respectively, whereas Os(1) is linked to four carbonyl ligands. The presence of the bridging hydride on the Os(2)–Os(3) edge was not observed crystallographically, but a significant distortion of the carbonyl and the phosphine ligands in the equatorial plane of the cluster strongly suggests its location. The bond angles Os(2)–Os(3)–C(31) and Os(3)–Os(2)–P of 108.4(4) and 115.8(1)° are much larger than the analogous Os(3)–Os(1)–C(13) and Os(1)–Os(3)–C(32) angles of 95.3(4) and 87.9(4)°. Moreover, the former angles in **2a** are similar to the corresponding angles of 111.2(1) and 120.5(1)° in the unsubstituted compound $(\mu\text{-H})\text{Os}_3(\text{CO})_{10}(\mu\text{-CH=CH}_2)$

**Figure 1.** View of the major isomer of $(\mu\text{-H})\text{Os}_3(\text{CO})_9(\text{PPh}_3)(\mu\text{-}\eta^2\text{-CH=CH}_2)$ (**2a**) perpendicular to the Os_3 plane.**Table 2. Selected Bond Distances (Å) for the Two Isomers of $(\mu\text{-H})\text{Os}_3(\text{CO})_9(\text{PPh}_3)(\mu\text{-}\eta^2\text{-CH=CH}_2)$ (**2a,b**)**

2a		2b	
Os(1)–Os(2)	2.9098(7)	Os(1)–Os(2)	2.857(1)
Os(2)–Os(3)	2.8616(7)	Os(2)–Os(3)	2.773(1)
Os(3)–Os(1)	2.8650(7)	Os(3)–Os(1)	3.137(1)
Os(2)–P	2.355(3)	Os(1)–P	2.382(5)
Os(1)–C(11)	1.90(2)	Os(1)–C(11)	1.84(2)
Os(1)–C(12)	1.95(1)	Os(1)–C(12)	1.92(2)
Os(1)–C(13)	1.89(2)	Os(1)–C(13)	1.96(2)
Os(1)–C(14)	1.95(2)	Os(2)–C(21)	1.87(2)
Os(2)–C(21)	1.89(2)	Os(2)–C(22)	1.90(2)
Os(2)–C(22)	1.89(1)	Os(2)–C(23)	1.92(3)
Os(3)–C(31)	1.91(1)	Os(3)–C(31)	1.93(2)
Os(3)–C(32)	1.88(1)	Os(3)–C(32)	1.86(2)
Os(3)–C(33)	1.91(1)	Os(3)–C(33)	1.86(2)
Os(2)–C(41)	2.32(1)	Os(3)–C(41)	2.28(2)
Os(2)–C(42)	2.25(1)	Os(3)–C(42)	2.26(2)
Os(3)–C(42)	2.12(1)	Os(2)–C(42)	2.09(2)
C(41)–O(11)	1.42(2)	C(41)–C(42)	1.49(3)
C(11)–O(11)	1.19(2)	C(11)–O(11)	1.17(3)
C(12)–O(12)	1.14(2)	C(12)–O(12)	1.17(3)
C(13)–O(13)	1.16(2)	C(13)–O(13)	1.12(3)
C(14)–O(14)	1.13(2)	C(21)–O(21)	1.14(3)
C(21)–O(21)	1.15(2)	C(22)–O(22)	1.14(3)
C(22)–O(22)	1.13(2)	C(23)–O(23)	1.11(3)
C(31)–O(31)	1.14(2)	C(31)–O(31)	1.13(3)
C(32)–O(32)	1.19(2)	C(32)–O(32)	1.15(3)
C(33)–O(33)	1.18(2)	C(33)–O(33)	1.16(3)
P–C(51)	1.81(2)	P–C(51)	1.83(2)
P–C(61)	1.86(1)	P–C(61)	1.83(2)
P–C(71)	1.83(1)	P–C(71)	1.82(2)

(1), in which the position of the hydride bridging the same edge as the vinyl moiety was determined by a combined X-ray and neutron diffraction study.⁶ In this comparison it is noteworthy that the replacement of a carbonyl with a triphenylphosphine ligand has little steric impact on the other carbonyl ligands. This is not unusual; for example, the structures of $(\mu\text{-H})_2\text{Os}_3(\text{CO})_{10}$ ^{7ab} and $(\mu\text{-H})_2\text{Os}_3(\text{CO})_9(\text{PPh}_3)$ ^{7c} correspond very closely.

The bridged Os(2)–Os(3) vector of 2.8616(7) Å is the shortest among the three metal-metal vectors, and the

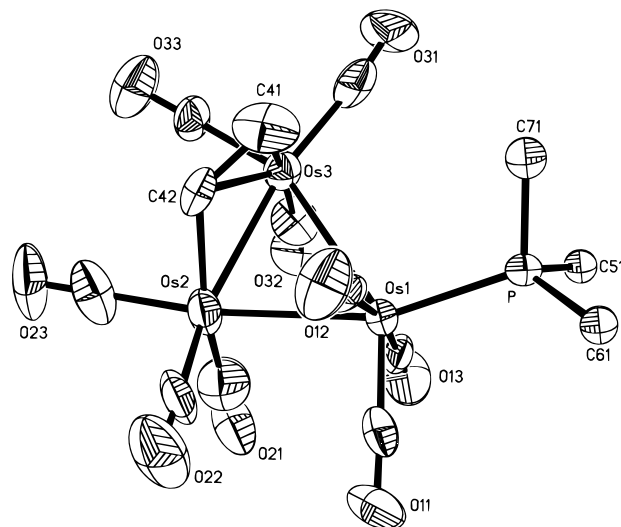
(6) (a) Orpen, A. G.; Rivera, V.; Bryan, E. G.; Pippard, D.; Sheldrick, G. M. *J. Chem. Soc., Chem. Commun.* **1978**, 723. (b) Orpen, A. G.; Pippard, D.; Sheldrick, G. M.; Rouse, K. D. *Acta Crystallogr.* **1978**, B34, 2466.

(7) (a) Broach, R. W.; Williams, J. M. *Inorg. Chem.* **1979**, 18, 314. (b) Churchill, M. R.; Hollander, F. J.; Hutchinson, J. P. *Inorg. Chem.* **1977**, 16, 2697. (c) Benfield, R. E.; Johnson, B. F. G.; Lewis, J.; Raithby, P. R.; Zuccaro, C. *Acta Crystallogr.* **1975**, B35, 2210.

Table 3. Selected Bond Angles (deg) for the Two Isomers of $(\mu\text{-H})\text{Os}_3(\text{CO})_9(\text{PPh}_3)(\mu\text{-}\eta^2\text{-CH}=\text{CH}_2)$ (2a,b**)**

2a		2b	
Os(1)–Os(2)–Os(3)	59.52(2)	Os(1)–Os(2)–Os(3)	67.72(3)
Os(2)–Os(3)–Os(1)	61.08(2)	Os(2)–Os(3)–Os(1)	57.41(3)
Os(3)–Os(1)–Os(2)	59.40(2)	Os(3)–Os(1)–Os(2)	54.87(3)
Os(3)–Os(1)–C(11)	96.4(5)	Os(3)–Os(1)–P	107.7(1)
Os(3)–Os(1)–C(12)	81.2(4)	Os(3)–Os(1)–C(11)	146.6(6)
Os(3)–Os(1)–C(13)	95.3(4)	Os(3)–Os(1)–C(12)	92.4(6)
Os(3)–Os(1)–C(14)	160.8(5)	Os(3)–Os(1)–C(13)	88.8(6)
Os(2)–Os(1)–C(11)	83.0(5)	Os(2)–Os(1)–P	159.3(1)
Os(2)–Os(1)–C(12)	91.2(4)	Os(2)–Os(1)–C(11)	92.3(6)
Os(2)–Os(1)–C(13)	153.4(5)	Os(2)–Os(1)–C(12)	77.6(6)
Os(2)–Os(1)–C(14)	103.5(5)	Os(2)–Os(1)–C(13)	94.5(5)
C(11)–Os(1)–C(12)	174.2(7)	P–Os(1)–C(11)	105.7(6)
C(11)–Os(1)–C(13)	92.7(7)	P–Os(1)–C(12)	93.5(6)
C(11)–Os(1)–C(14)	89.5(7)	P–Os(1)–C(13)	96.3(5)
C(12)–Os(1)–C(13)	92.9(7)	C(11)–Os(1)–C(12)	85.7(9)
C(12)–Os(1)–C(14)	91.1(6)	C(11)–Os(1)–C(13)	87.5(9)
C(13)–Os(1)–C(14)	102.8(7)	C(12)–Os(1)–C(13)	169.3(8)
Os(3)–Os(2)–P	115.83(8)	Os(3)–Os(2)–C(21)	104.6(8)
Os(3)–Os(2)–C(21)	138.3(4)	Os(3)–Os(2)–C(22)	150.7(7)
Os(3)–Os(2)–C(22)	110.2(4)	Os(3)–Os(2)–C(23)	102.8(7)
Os(3)–Os(2)–C(41)	71.6(3)	Os(3)–Os(2)–C(42)	53.1(6)
Os(3)–Os(2)–C(42)	47.1(3)	Os(1)–Os(2)–C(21)	86.5(8)
Os(1)–Os(2)–P	159.64(8)	Os(1)–Os(2)–C(22)	93.8(6)
Os(1)–Os(2)–C(21)	94.8(4)	Os(1)–Os(2)–C(23)	170.2(7)
Os(1)–Os(2)–C(22)	75.2(4)	Os(1)–Os(2)–C(42)	90.0(5)
Os(1)–Os(2)–C(41)	113.5(3)	C(21)–Os(2)–C(22)	96.3(10)
Os(1)–Os(2)–C(42)	77.5(3)	C(21)–Os(2)–C(23)	94(1)
P–Os(2)–C(21)	99.0(4)	C(21)–Os(2)–C(42)	156.7(9)
P–Os(2)–C(22)	89.5(4)	C(22)–Os(2)–C(42)	106.9(9)
P–Os(2)–C(41)	80.6(3)	C(22)–Os(2)–C(23)	95.9(9)
P–Os(2)–C(42)	114.8(3)	C(23)–Os(2)–C(42)	86.0(10)
C(21)–Os(2)–C(41)	91.4(6)	Os(2)–Os(3)–C(31)	165.1(6)
C(21)–Os(2)–C(42)	93.6(6)	Os(2)–Os(3)–C(32)	89.4(7)
C(21)–Os(2)–C(42)	98.6(5)	Os(2)–Os(3)–C(33)	97.6(6)
C(22)–Os(2)–C(41)	169.6(5)	Os(2)–Os(3)–C(41)	80.6(6)
C(22)–Os(2)–C(42)	151.6(5)	Os(2)–Os(3)–C(42)	47.8(5)
C(41)–Os(2)–C(42)	36.0(4)	Os(1)–Os(3)–C(31)	108.9(6)
Os(1)–Os(3)–C(31)	168.9(4)	Os(1)–Os(3)–C(32)	88.8(6)
Os(1)–Os(3)–C(32)	87.9(4)	Os(1)–Os(3)–C(33)	155.0(6)
Os(1)–Os(3)–C(33)	97.9(4)	Os(1)–Os(3)–C(41)	81.0(5)
Os(1)–Os(3)–C(42)	80.6(4)	Os(1)–Os(3)–C(42)	80.2(5)
Os(2)–Os(3)–C(31)	108.4(4)	C(31)–Os(3)–C(32)	96.6(9)
Os(2)–Os(3)–C(32)	135.3(4)	C(31)–Os(3)–C(33)	95.8(9)
Os(2)–Os(3)–C(33)	119.2(5)	C(31)–Os(3)–C(41)	91.9(8)
Os(2)–Os(3)–C(42)	51.2(3)	C(31)–Os(3)–C(42)	128.8(8)
C(31)–Os(3)–C(32)	98.8(6)	C(32)–Os(3)–C(33)	92.2(9)
C(31)–Os(3)–C(33)	90.3(6)	C(32)–Os(3)–C(41)	168.4(8)
C(31)–Os(3)–C(42)	90.0(5)	C(32)–Os(3)–C(42)	134.5(8)
C(32)–Os(3)–C(33)	94.7(6)	C(33)–Os(3)–C(41)	94.8(8)
C(32)–Os(3)–C(42)	95.3(5)	C(33)–Os(3)–C(42)	81.3(8)
C(33)–Os(3)–C(42)	169.8(5)	C(41)–Os(3)–C(42)	38.3(8)
Os(2)–C(41)–C(42)	69.5(7)	Os(3)–C(41)–C(42)	70(1)
Os(2)–C(42)–Os(3)	81.6(4)	Os(2)–C(42)–Os(3)	79.1(7)
Os(2)–C(42)–C(41)	74.5(7)	Os(2)–C(42)–C(41)	133(1)
Os(3)–C(42)–C(41)	118.7(9)	Os(3)–C(42)–C(41)	72(1)

Os(1)–Os(2) vector of 2.9098(7) Å is longer than the Os(1)–Os(3) vector of 2.8650(7) Å. Both of these aspects are consistent with results found in the other crystallographically analyzed hydrido μ,η^2 -alkenyl clusters, namely $(\mu\text{-H})\text{Os}_3(\text{CO})_{10}(\mu,\eta^2\text{-trans-CH}=\text{CHR})$ (R = H,⁵ Et,^{8a} ^tBu^{8b}), $(\mu\text{-H})\text{Os}_3(\text{CO})_{10}(\mu,\eta^2\text{-cis-CPh}=\text{CHPh})$,⁹ $(\mu\text{-SPh})\text{Os}_3(\text{CO})_{10}(\mu,\eta^2\text{-CH}=\text{CH}_2)$,¹⁰ and $(\mu\text{-Br})\text{Os}_3(\text{CO})_{10}(\mu,\eta^2\text{-trans-CH}=\text{CHPh})$.¹¹ The orientation of the hydrogen atom on the α -carbon of the vinyl moiety in **2a** is

**Figure 2.** View of the minor isomer of $(\mu\text{-H})\text{Os}_3(\text{CO})_9(\text{PPh}_3)(\mu\text{-}\eta^2\text{-CH}=\text{CH}_2)$ (**2b**) perpendicular to the Os_3 plane.

syn with respect to the $\text{Os}(\text{CO})_4$ unit. This orientation is the same as that of $(\mu\text{-H})\text{Os}_3(\text{CO})_{10}(\mu,\eta^2\text{-CH}=\text{CHR})$ (R = H,⁵ Et,^{8a} ^tBu^{8b}) and $(\mu\text{-SPh})\text{Os}_3(\text{CO})_{10}(\mu,\eta^2\text{-CH}=\text{CH}_2)$.¹⁰ The carbon–carbon bond distance of 1.42(2) Å in the vinyl moiety is marginally longer than that of 1.396(2) Å in **1**⁶ and significantly longer than expected for a normal carbon–carbon double bond of 1.33 Å.¹² The Os(2)–C(41) and Os(2)–C(42) distances of 2.32(1) and 2.25(1) Å involving the π -bond are shorter than those of 2.362(3) and 2.273(3) Å in **1**, respectively.⁶ These findings imply an enhanced interaction between the vinyl moiety π -bonded to the osmium center that also bears the phosphorus ligand.

Crystal Structure of 2b. An ORTEP diagram of the molecular configuration determined for **2b** is shown in Figure 2. Selected bond distances and angles are tabulated in Tables 2 and 3, respectively. The cluster contains a triangular array of osmium atoms, but its structure (configuration C) differs from the previously proposed structure (configuration B).³ The phosphine ligand is located in an equatorial position on Os(1). The vinyl ligand bridges the Os(2)–Os(3) edge, forming a σ -bond to Os(2) and a π -bond to Os(3). Each of the three metal atoms is associated with three terminal carbonyl ligands.

The presence of a bridging hydride on the Os(1)–Os(3) edge was detected at an intermediate stage of refinement, but the location did not converge in the final analysis with the full diffraction set. However, the Os(1)–Os(3) distance of 3.137(1) Å is significantly longer than the average metal–metal distance of 2.877 Å in $\text{Os}_3(\text{CO})_{12}$,¹³ and this increase is consonant with the observation that the addition of a single bridging hydride ligand to an unsupported metal–metal bond increases the metal–metal bond distance.¹⁴ Further support for the location of the hydride ligand is provided by the widened angles of Os(1)–Os(3)–C(31) and Os(3)–Os(1)–P of 108.9(6) and 107.7(1)°, compared with the corresponding angles of 90.2(1) and 100.8(1)° found in **1**.⁶

(8) (a) Guy, J. J.; Reichert, B. E.; Sheldrick, G. M. *Acta Crystallogr.* **1976**, B32, 3319. (b) Sappa, E.; Tiripicchio, A.; Lanfredi, A. M. M. *J. Organomet. Chem.* **1983**, 249, 391.

(9) Clauss, A. D.; Tachikawa, M.; Shapley, J. R.; Pierpont, C. G. *Inorg. Chem.* **1981**, 20, 1528.

(10) Boyar, E.; Deeming, A. J.; Henrick, K.; McPartlin, M.; Scott, A. *J. Chem. Soc., Dalton Trans.* **1986**, 1431.

(11) Chi, Y.; Chen, B.-F.; Wang, S.-L.; Chiang, R.-K.; Hwang, L.-S. *J. Organomet. Chem.* **1989**, 377, C59.

(12) Bartel, L. S.; Bonham, R. A. *J. Chem. Phys.* **1960**, 32, 824.

(13) Churchill, M. R.; DeBoer, B. G. *Inorg. Chem.* **1977**, 16, 878.

(14) (a) Churchill, M. R.; DeBoer, B. G.; Rotella, F. J. *Inorg. Chem.* **1976**, 15, 1843. (b) Churchill, M. R. *Adv. Chem. Ser.* **1978**, No. 167, 36.

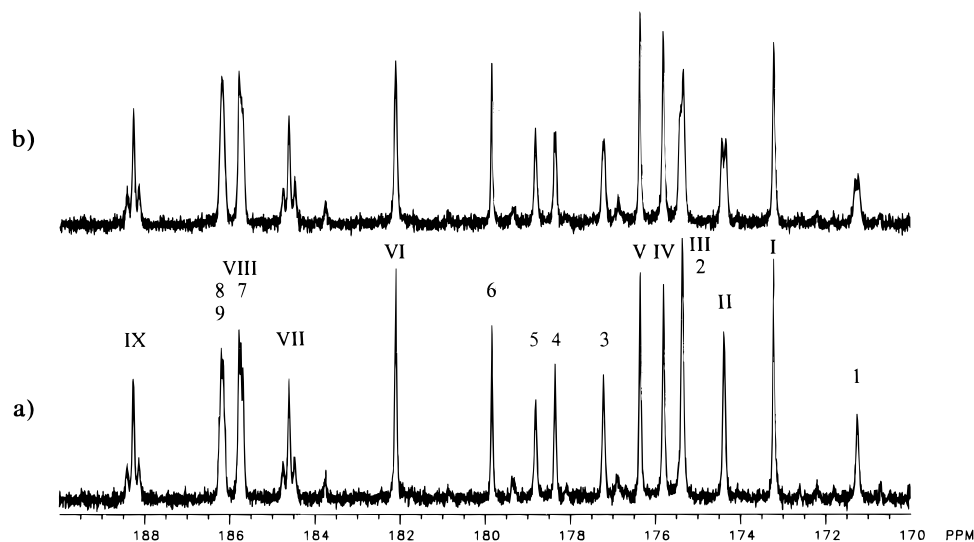


Figure 3. ^{13}C NMR spectra of the two isomers **2a** and **2b** at -70°C in toluene- d_8 : (a) ^1H decoupled; (b) ^1H coupled.

The Os(2)–Os(3) vector, which is bridged by the vinyl ligand, is only 2.773(1) Å, which is substantially shorter than the corresponding distances of 2.845(2) and 2.8616(7) Å in **1** and **2a**, respectively. This shortened metal–metal distance in **2b** is consistent with the absence of the hydride ligand on the edge bridged by the vinyl moiety. The other crystallographically analyzed triosmium hydrido alkenyl clusters contain the hydride in the same edge as the alkenyl moiety;^{6,8,9} there are scores of compounds with the general formula $(\mu\text{-H})\text{Os}_3(\text{CO})_{10}(\mu\text{-X})$, where X is a three-electron bridging ligand, that also have a bridging hydride on the same edge.¹ This is true for the dithioformate compound $(\mu\text{-H})\text{Os}_3(\text{CO})_9(\mu, \eta^2\text{-SCHS})$ but not true for the phosphine derivative $(\mu\text{-H})\text{Os}_3(\text{CO})_8(\text{PMe}_2\text{Ph})(\mu, \eta^2\text{-SCHS})$.^{2a,b} In the latter compound the hydride does not bridge the same edge as the dithioformate ligand, the phosphine ligand is bonded to the osmium atom that does not coordinate to the dithioformate ligand, and the phosphine is also located cis to the bridging hydride. However, the effect of phosphine substitution cannot be generalized, since in either $(\mu\text{-H})(\mu, \eta^2(N, O)\text{-CH}_3\text{C}_6\text{H}_4\text{NCHO})\text{Os}_3(\text{CO})_{10}$ or its phosphine-substituted analog the bridging hydride shares the same edge as the bridging formamide ligand.^{2c} Moreover, in each of the compounds $(\mu\text{-H})(\mu\text{-}\eta^2\text{-}(\text{CF}_3)\text{-C}=\text{NH})\text{Os}_3(\text{CO})_9(\text{L})$ (L = CO, PMe_2Ph) and $(\mu\text{-H})(\mu\text{-}\eta^1\text{-N}=\text{C}(\text{H})\text{CF}_3)\text{Os}_3(\text{CO})_9(\text{L})$ (L = CO, PMe_2Ph), the hydride ligand shares the same edge as the other bridging ligands.^{2d}

The carbon–carbon bond distance in the vinyl moiety of **2b** is 1.49(3) Å, which is significantly longer than the previously reported values of 1.36–1.40 Å in analogous μ, η^2 hydrido alkenyl clusters^{6,8,9} and of 1.42(2) Å in **2a**. The Os(3)–C(41) and Os(3)–C(42) distances are 2.28(2) and 2.26(2) Å, respectively, which are significantly shorter than the reported values of 2.36–2.46 and 2.27–2.28 Å, respectively, in related μ, η^2 hydrido alkenyl clusters.^{6,8,9} However, the two carbon atoms in the vinyl moiety as well as Os(2) show anomalous thermal motion, probably caused by local disorder, which could not be resolved. The disorder might arise from a small fraction of another isomer that possesses a structure in which the vinyl moiety has a σ -bond to Os(3) and a π -bond to Os(2). This species may contribute to the dynamic behavior of **2b** in solution (*vide infra*).

In **2b** the orientation of the hydrogen atom on the α -carbon of the vinyl moiety is anti or away from the $\text{Os}(\text{CO})_3(\text{PPh}_3)$ unit. This orientation is the same as that seen in $(\mu\text{-H})\text{Os}_3(\text{CO})_{10}(\mu, \eta^2\text{-cis-CPh}=\text{CHPh})$ ⁹ and $(\mu\text{-Br})\text{Os}_3(\text{CO})_{10}(\mu, \eta^2\text{-trans-CH}=\text{CHPh})$.¹¹ While these anti-oriented clusters appear to adopt their orientation due to steric hindrance of the alkenyl moieties, this is not obviously the case with **2b**. One hypothesis to explain the difference between **2b** and **2a** involves the reaction pathway to interconvert the two isomers, as discussed below.

Solution Structures of 2a and 2b. The ^{13}C NMR spectrum (at 125 MHz) of ca. 40% ^{13}C -enriched $(\mu\text{-H})\text{Os}_3(\text{CO})_9(\text{PPh}_3)(\mu, \eta^2\text{-CH}=\text{CH}_2)$ in toluene- d_8 at -70°C displays 15 carbonyl resonances (Figure 3) due to the presence of both **2a** and **2b**. Each of the isomers has nine carbonyl resonances with equal intensities, but some of the resonances happen to overlap at this temperature. The two isomers were present in the ratio of 2.2:1. A combination of ^{13}C experiments allowed assignment of the carbonyl signals and elucidation of the solution structures for both isomers. Proceeding downfield, the resonances are designated from I to IX for **2a** and from 1 to 9 for **2b**. The ^{13}C NMR data are summarized in Table 4 and the assignments are shown in Chart 1.

A starting point for the assignment of each isomer is the the pair of trans axial carbonyls, which typically display unique patterns due to relatively large values of $^2J(\text{CC})$ (ca. 35 Hz).^{15,16} For **2a**, examination of resonances VII and IX shows that they are singlets overlapped with a doublet ($^2J(\text{CC}) = 36$ Hz) due to the partial ^{13}C incorporation (ca. 40%). For **2b** the trans axial carbonyls correspond to resonances 8 and 9, which are not resolved at -70°C . However, the two patterns separate at higher temperatures (*vide infra*), and each resonance shows phosphorus coupling of 5.2 Hz. This is a typical value for a two-bond cis coupling between a carbonyl and a phosphine ligand in triosmium clus-

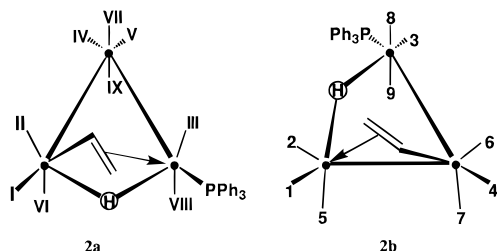
(15) (a) Tachikawa, M.; Richter, S. I.; Shapley, J. R. *J. Organomet. Chem.* **1977**, *123*, C9. (b) Aime, S.; Gobetto, R.; Milone, K.; Rosenberg, E.; Ansllyn, E. V. *Inorg. Chim. Acta* **1986**, *111*, 95.

(16) (a) Cree-Uchiyama, M.; Shapley, J. R.; St. George, G. M. *J. Am. Chem. Soc.* **1986**, *108*, 1316. (b) Chi, Y.; Shapley, J. R.; Churchill, M. R.; Li, Y.-J. *Inorg. Chem.* **1986**, *25*, 4165. (c) Park, J. T.; Shapley, J. R.; Churchill, M. R.; Bueno, C. *Inorg. Chem.* **1983**, *22*, 1579.

Table 4. ¹³C NMR Data for the Two Isomers of (μ -H)Os₃(*CO)₉(PPh₃)(μ - η^2 -CH=CH₂) (**2a,b**)^a

signal	chem shift ^b δ (ppm)	coupling consts (Hz) ^b		
		<i>J</i> (CH)	<i>J</i> (CP)	<i>J</i> (CC)
Compound 2a				
I	173.2	w		
II	174.4	12.8		
III	175.4	9.2	w	
IV	175.8			
V	176.4			
VI	182.1	w		
VII	184.6			36
VIII	185.8	w	5.4 ^c	
IX	188.3			36
Compound 2b				
1	171.2	8.6		
2	174.4	w		
3	177.2	7.0		
4	178.4	4.3 ^d		
5	178.8	w		
6	179.8			
7	185.8			
8	186.2		5.2 ^c	35 ^c
9	186.2		5.2 ^c	35 ^c

^a At -70 °C unless noted otherwise; toluene-*d*₈. ^b w indicates a small unresolved coupling. ^c Measured at -30 °C. ^d Coupling due to vinyl proton (see text).

Chart 1

ters,¹⁷ and it clearly indicates that the triphenylphosphine ligand is associated with the same osmium atom as the trans axial carbonyls. This conclusion is consistent with the X-ray structure of **2b** (Figure 2).

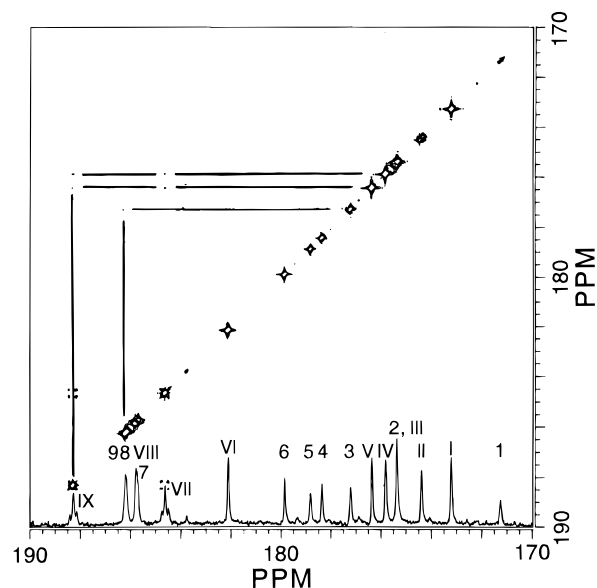
The ¹³C{¹H}-COSY spectrum of ¹³CO-enriched **2a/2b** in toluene-*d*₈ at -70 °C is shown in Figure 4. For a triosmium carbonyl cluster only two-bond couplings normally appear in the cross peaks; in other words, the two resonances that are linked by an off-diagonal peak correspond to two carbonyls coordinated to the same osmium atom.^{18–20} In the observed spectrum both resonances IV and V are coupled to both resonances VII and IX. Therefore, since VII and IX are assigned to the trans axial carbonyls on the Os(CO)₄ unit, IV and V are assigned to the corresponding equatorial carbonyls. In **2b** isochronous resonances 8 and 9, assigned to the transaxial carbonyls, show cross peaks to resonance 3, which then is assigned to the equatorial carbonyl on the Os(CO)₃(PPh₃) unit.

(17) (a) Gallop, M. A.; Johnson, B. F. G.; Khattar, R.; Lewis, J.; Raithby, P. R. *J. Organomet. Chem.* **1990**, *386*, 121. (b) Rosenberg, E.; Bracker-Novak, J.; Gelbert, R. W.; Aime, S.; Gobetto, R.; Osella, D. *J. Organomet. Chem.* **1989**, *365*, 163. (c) Farrugia, L. J. *Organometallics* **1989**, *8*, 2410. (d) Ewing, P.; Farrugia, L. J. *Organometallics* **1989**, *8*, 1665. (e) Martin, L. R.; Einstein, F. W. B.; Pomeroy, R. K. *Organometallics* **1988**, *7*, 294. (f) Keister, J. B.; Shapley, J. R. *Inorg. Chem.* **1982**, *21*, 3304. (g) Martin, L. R.; Einstein, F. W. B.; Pomeroy, R. K. *Organometallics* **1988**, *7*, 294.

(18) Hawkes, G. E.; Lian, L. Y.; Randall, E. W.; Sales, K. D. *J. Chem. Soc., Dalton Trans.* **1985**, 225.

(19) Aime, S.; Osella, D. *J. Chem. Soc., Chem. Commun.* **1981**, 300.

(20) Ewing, P.; Farrugia, L. J.; Rycroft, D. S. *Organometallics* **1988**, *7*, 859.

**Figure 4.** ¹³C{¹H}-COSY spectrum of the two isomers **2a** and **2b** at -70 °C in toluene-*d*₈.

Further insight was gained by consideration of ¹H-coupled ¹³C NMR spectra (Figure 3). None of the carbonyl resonances on the Os(CO)₄ unit in **2a** show any coupling to the hydride ligand, whereas the remaining five resonances do show such interactions. Thus, the hydride ligand is in the bridged position on the edge between the Os(CO)₃ and Os(CO)₂(PPh₃) units, consistent with the solid state structure of **2a** (Figure 1). Resonances II and III are strongly coupled to the carbonyls located in a trans position. Since III appears at lower field than II, it likely corresponds to the carbonyl on the Os(CO)₂(PPh₃) unit.^{17a,21} Resonance VIII is coupled to a phosphorus nucleus by 5.4 Hz, which is a typical value for ²*J*(CP_{cis}) in related clusters;¹⁷ thus, this resonance is assigned to the carbonyl in the remaining pseudo-axial position on the Os(CO)₂(PPh₃) unit. Resonances I and VI correspond to the two remaining carbonyls on the Os(CO)₃ unit, with I likely corresponding to the carbonyl in the equatorial position.¹⁶

The carbonyl resonances of **2b** are assigned in a similar way. Comparison of the proton-coupled and decoupled spectra in Figure 3 reveals weak proton coupling for resonances 2 and 5 and strong coupling for resonances 1, 3, and 4. Since resonance 3 is assigned to the equatorial carbonyl on the Os(CO)₃(PPh₃) unit, the hydride ligand is clearly linked to the Os(CO)₃(PPh₃) unit. One of the Os(CO)₃ units is also linked to the bridging hydride, and resonance 1 is assigned to the carbonyl on this unit trans to the bridging site. Resonances 2 and 5, which show weak coupling to the hydride, are then assigned to the carbonyls in the equatorial and the pseudo-axial positions, respectively, on this unit.

The remaining three resonances, 4, 6, and 7, belong to the final Os(CO)₃ unit. An initially puzzling observation is that resonance 4 shows proton coupling of 4.3

(21) (a) Chi, Y.; Shapley, J. R.; Ziller, J. W.; Churchill, M. R. *Organometallics* **1987**, *6*, 301. (b) Chi, Y.; Shapley, J. R.; Churchill, M. R.; Fettinger, J. C. *J. Organomet. Chem.* **1989**, *372*, 273. (c) Alex, R. F.; Pomeroy, R. K. *Organometallics* **1987**, *6*, 2437. (d) Alex, R. F.; Pomeroy, R. K. *J. Organomet. Chem.* **1985**, *284*, 379. (e) Johnson, B. F. G.; Lewis, J.; Reichert, B. E.; Schorpp, K. T. *J. Chem. Soc., Dalton Trans.* **1976**, 1403.

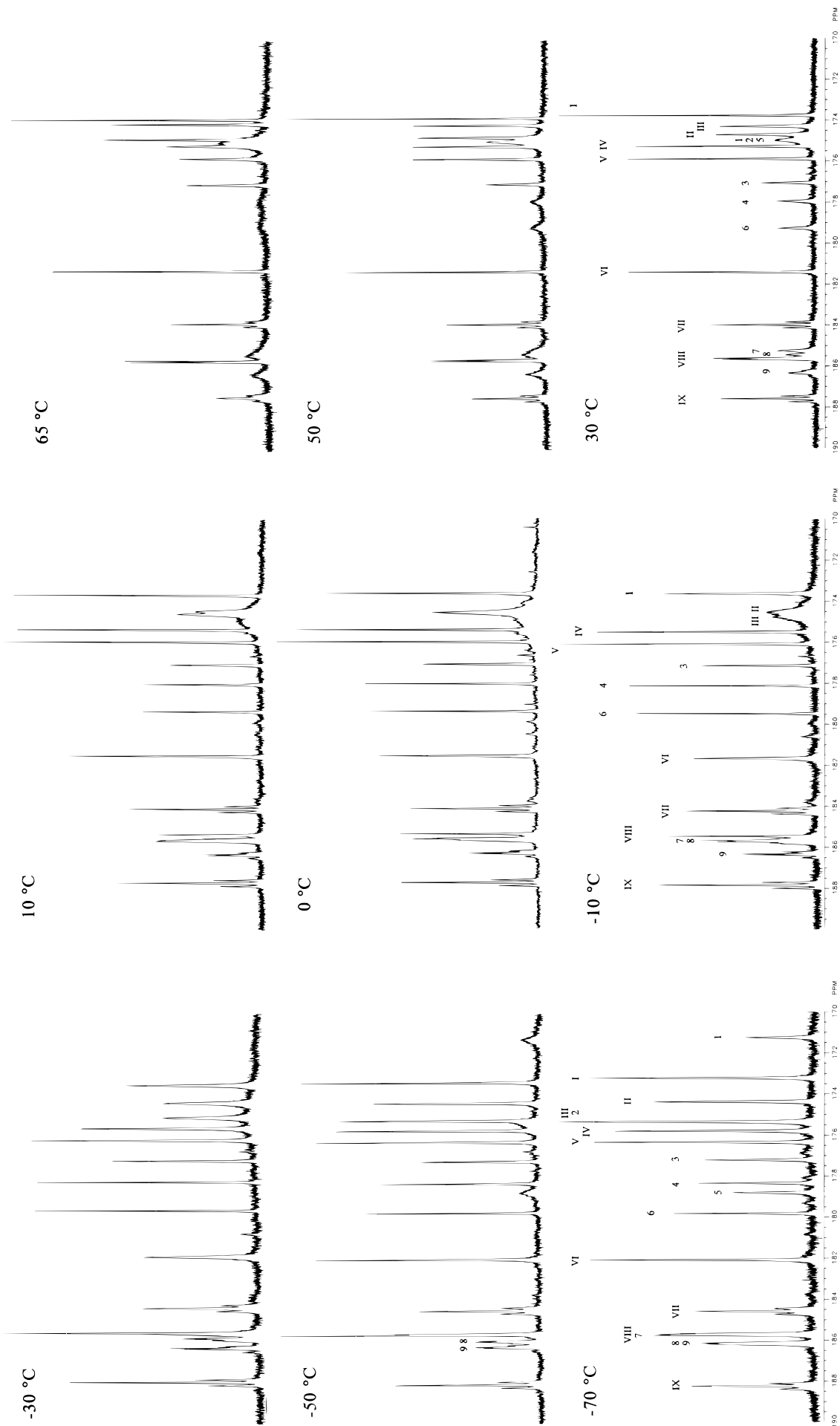


Figure 5. Variable-temperature ^{13}C NMR spectra of the two isomers **2a** and **2b**.

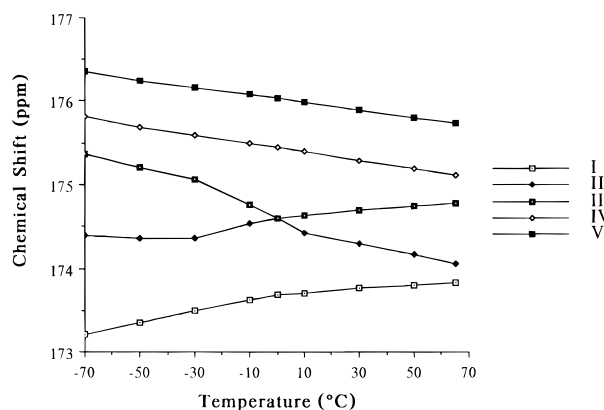


Figure 6. Temperature dependence of the chemical shifts of five carbonyl ^{13}C NMR resonances in **2a**.

Hz. However, selective ^1H -decoupled ^{13}C NMR experiments showed that this was due to a proton in the vinyl group (see Figure S-1 in the Supporting Information). Upon irradiation of the proton on the α -carbon of the vinyl moiety (H_α), the doublet of resonance 4 collapsed, whereas the broad singlet of resonance 3 remained virtually the same. On the other hand, upon the irradiation of the hydride resonance, the broad singlet of resonance 3 became sharper and resonance 4 was unaffected. Therefore, the splitting of resonance 4 is caused by H_α on the vinyl moiety, which we can assume is σ -bonded to this $\text{Os}(\text{CO})_3$ unit. The carbonyl generating resonance 4 must have a special spatial relationship with the vinyl $\text{C}\text{-H}_\alpha$ bond. Inspection of Figure 2 suggests that the equatorial carbonyl ($\text{C}(23)\text{-O}(23)$) trans to the unsupported metal–metal bond should be nearly coplanar with this $\text{C}\text{-H}_\alpha$ vector, whereas the other two carbonyls are positioned in a nearly perpendicular plane. Since resonance 7 is significantly shifted downfield, it is assigned to the more nearly axial position on this osmium center. Once again, the solution structure of this isomer, as deduced from the ^{13}C NMR spectra, is fully consistent with that of the corresponding single-crystal X-ray analysis.

Dynamic Behavior of Isomers 2a and 2b. Variable-temperature ^{13}C NMR spectra of the **2a/2b** mixture in toluene- d_8 were recorded from -70 to $+65$ °C (Figure 5). The behavior of the two signals II and III for **2a** is conspicuously anomalous. From -70 to -10 °C the two resonances gradually broaden at the same rate and finally coalesce to one broad resonance at 0 °C. In contrast, over the same temperature range resonances I, VI, and VIII in **2a** broaden, but not as much as II and III. When the temperature is raised to 10 °C, the very broad resonance due to II/III again becomes *two* broad resonances. As the temperature is raised further, the line width of each of the two resonances becomes narrower at the same rate, and they continue to diverge. In the same temperature range, resonances I, VI, and VII become narrower, also. All of the resonances that change line width correspond to the carbonyls bonded to the two osmium atoms bridged by the hydride and the vinyl moiety. The chemical shifts of selected resonances in **2a** are plotted against temperature in Figure 6. As the temperature increases, the chemical shifts of II and III move in opposite directions and cross each other at 0 °C.

To clarify whether the carbonyls corresponding to signals II and III are exchanging with each other, ^{13}C spin saturation transfer experiments were performed

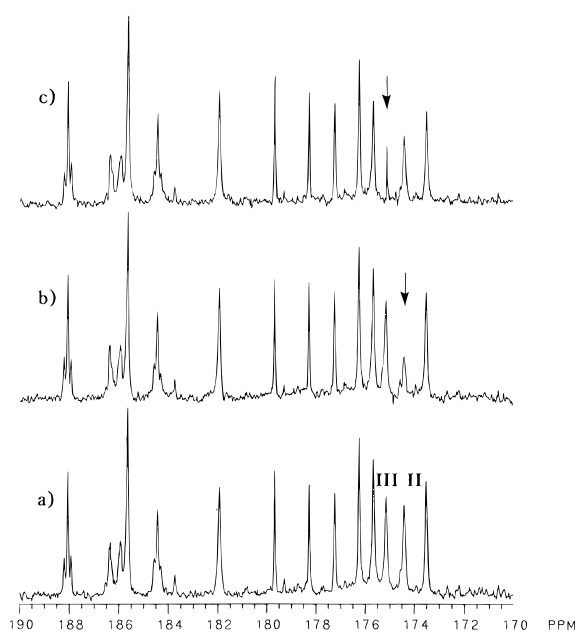


Figure 7. ^{13}C spin saturation transfer experiments for **2a**: (a) reference spectrum; (b) spectrum where signal II was irradiated; (c) spectrum where signal III was irradiated.

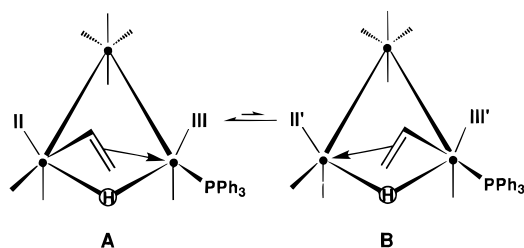
at -30 °C. The results are shown in Figure 7. The irradiation of either carbonyl signal II or III did not cause any significant decrease in intensity of the other. The T_1 relaxation time of either resonance II or III at -30 °C was measured as 500 ± 100 ms. The line width of either resonance II or III increases by ca. 9 Hz from -70 to -30 °C, indicating the rate of exchange, k , is ca. 9π or 27 s^{-1} at -30 °C. Since the relaxation rate constant, ρ , can be approximated as the inverse of the T_1 relaxation time,²² the relative signal intensity of one resonance upon irradiation of its exchange partner would be $\rho/(\rho + k) = 2/(27+2) = 0.1$. These results clearly show that the two carbonyls are not exchanging with each other; therefore, they must be exchanging with carbonyl sites in a separate “unseen” partner species.

The spectral behavior observed for **2a** from -70 to $+30$ °C is readily explained on the basis of σ/π interchange in the vinyl group. At low temperatures only configuration A, as found in the solid-state, is detected in the solution ^{13}C NMR spectra. As the temperature increases, an increasing amount of configuration B forms, and the carbonyl resonances of the major form A appear to become broader due to the rapid σ/π interchange involving the vinyl moiety. Each of the observed chemical shifts is the population-weighted average of the chemical shifts in the individual configurations A and B (see Scheme 1). Interchange of the vinyl bonds would be expected to most strongly affect the chemical shifts of carbonyls II and III trans to the hydride ligand, since these sites were the most widely separated (7 ppm) in the parent compound **1**.⁴ The overlap observed at 0 °C is due coincidentally to the fact that the weighted average of resonances II and II' is the same as the average of III and III'. As shown above, there is no direct dynamic link between sites II and III.

It is not possible to completely eliminate tripod rotation in the $\text{Os}(\text{CO})_2\text{PPh}_3$ moiety as the source of the

(22) Campbell, I. D.; Dobson, C. M.; Ratcliffe, R. G.; Williams, R. J. *P. J. Magn. Reson.* **1978**, *29*, 397.

Scheme 1



unseen partner for **2a**, since both exchanging forms cannot be observed directly.^{23,24} Nevertheless, it is unlikely that such tripodal isomers would have the well-separated chemical shifts needed to explain the observed behavior. Exchange involving the Os(CO)₄ unit becomes observable above 30 °C as resonances IV, V, VII, and IX lose intensity due to broadening. The hint that IX broadens faster than VII is consistent with other observations that the two inequivalent (ax, eq, eq) triad combinations can undergo local exchange at different rates.^{25,26}

Isomer **2b** also undergoes dynamic behavior that is visible in the variable-temperature ¹³C NMR spectra (see Figure 5). From -70 to -10 °C, resonances 1, 2, and 5 broaden at the same rate and disappear into the base line. At 10 °C a very broad resonance appears at 174.7 ppm, which is close to the calculated mean, and this resonance sharpens at higher temperatures. Since the corresponding carbonyl ligands belong to the same Os(CO)₃ unit, specifically the one also π-bonded to the vinyl moiety, this process clearly involves local 3-fold carbonyl exchange at this center. Analogous behavior is seen for the other Os(CO)₃ unit linked to the vinyl group, but in this case the corresponding resonances 4, 6, and 7 broaden over the temperature range from 30 to 65 °C. Faster Os(CO)₃ exchange at the center π-bonded to the μ-vinyl group was also determined in a detailed recent study of a diosmium compound.²⁴

In the temperature range of 30–65 °C, resonances 8 and 9 as well as the coalesced 1, 2, 5 signal also are observed to broaden, but to a smaller extent than the 4, 6, 7 group. Only resonance 3 for the carbonyl trans to the hydride appears to be unaffected. The dynamic behavior responsible for these latter effects cannot be assigned in detail, but it may also involve σ/π interchange in the vinyl group. If so, it appears that this process has a higher energy barrier in **2b** than in **2a**.

Formation and Interconversion of Isomers 2a and 2b. The interaction of simple Lewis bases (L) with (μ-H)₂Os₃(CO)₁₀ produces adducts of the formula (μ-H)-HOs₃(CO)₁₀L, where the terminal hydride ligand and L are bound to two separate Os(CO)₃ centers connected by the bridging hydride ligand.²⁷ When one of the initial osmium centers is substituted, as in (μ-H)₂Os₃(CO)₉PPh₃, then coordination of L could produce two isomeric

adducts, depending on which center is attacked. Brown and Evans³ suggested that addition of nucleophiles to the unsaturated Os(μ-H)₂Os moiety should be subject to frontier orbital control and that donor ligand substitution on one Os center should generate a LUMO with greater amplitude at that center. Indeed, they showed that methyl isocyanide, a sterically undemanding ligand, preferentially coordinates to the substituted osmium center. However, our observation that isomers **2a** and **2b** are in equilibrium clearly shows that their formation is not directly linked to the relative stabilities of isomeric initial adducts. Hidden rearrangements are likely involved in the insertion reactions of (μ-H)₂Os₃(CO)₉L with other unsaturated substrates.^{2a–d,f,m}

The rearrangement pathway connecting **2a** and **2b** must involve CO migration and likely involves migration of vinyl linkages as well. A compact pathway would involve structure B, generated from the ground-state structure A for isomer **2a** by the σ,π-vinyl interchange discussed above. Then, carbonyl migration coupled with migration of the vinyl σ-bond on the same edge, passing through a (μ-CO, μ-σ-CH) configuration, would give directly structure C, as observed for **2b**. Further studies of this interconversion as a function of the phosphine ligand are underway, and these may reveal more details about the rearrangement pathway.

We have shown earlier^{2m} that the observed product from the reaction of (μ-H)₂Os₃(CO)₉PPh₃ with ethylene is the ethylidene compound (μ-H)Os₃(CO)₉(PPh₃)(μ-CHCH₃) instead of the ethylene complex (μ-H)Os₃(CO)₉(PPh₃)(C₂H₄) claimed by Brown and Evans.³ We have now shown that the ethylidene complex reacts with ethylene at higher pressures to give the vinyl complex isomers **2a** and **2b**. The overall transformation parallels the reaction of the unsubstituted compound (μ-H)₂Os₃(CO)₁₀ with ethylene to give vinyl complex **1**,^{4b} for which equilibrating ethyl and ethylidene intermediates were subsequently characterized.^{16a} The ethyl complex (μ-H)Os₃(CO)₁₀(μ-CH₂CH₃) is the species that actually reacts with ethylene, resulting in reductive elimination of ethane and C–H insertion to form **1**. It is likely that an analogous ethyl species is involved in the reaction of ethylene with (μ-H)₂Os₃(CO)₉PPh₃, although it was not observed in the previous solution NMR study of (μ-H)Os₃(CO)₉(PPh₃)(μ-CHCH₃).^{2m}

Acknowledgment. This work was supported by grants from the National Science Foundation (Grant No. CHE 94-14217 and predecessors). M.K. thanks the Sankei Scholarship Foundation, the University of Illinois, and the Walter Brown Endowment Fund for fellowships. We thank Dr. Vera Mainz for setting up the ¹³C spin saturation transfer experiments.

Supporting Information Available: Details of the X-ray crystallographic studies of **2a** and **2b** together with tables of all positional parameters, thermal parameters, and refined distances and angles and a figure giving ¹³C selectively ¹H-decoupled NMR spectra of **2a/2b** at -70 °C (17 pages). Ordering information is given on any current masthead page.

OM9607006

(23) Chuang, S.-H.; Chi, Y.; Liao, F.-L.; Wang, S.-L.; Peng, S.-M.; Lee, G.-H.; Wu, J.-C.; Horng, K.-M. *J. Organomet. Chem.* **1991**, *12*, 1616.

(24) Farrugia, L. J.; Chi, Y.; Tu, W.-C. *Organometallics* **1993**, *12*, 1616.

(25) Park, J. T.; Shapley, J. R.; Churchill, M. R.; Bueno, C. *Inorg. Chem.* **1983**, *22*, 1579.

(26) Gavens, P. D.; Mays, M. J. *J. Organomet. Chem.* **1978**, *162*, 389.

(27) (a) Shapley, J. R.; Keister, J. B.; Churchill, M. R.; DeBoer, B. G. *J. Am. Chem. Soc.* **1975**, *97*, 4145. (b) Deeming, A. J.; Hasso, S. J. *Organomet. Chem.* **1975**, *88*, C21.